EURASIP Journal on Applied Signal Processing 2005:1, 20–29

Adaptive Denoising and Equalization of Infrared Wireless CDMA System

Xavier N. Fernando
Advanced Radio-Optics Integrated Technology Group (ADROIT), Ryerson University, Toronto, Canada M5B 2J1
Email: xavier@ieee.org

Balakanthan Balendran
Advanced Radio-Optics Integrated Technology Group (ADROIT), Ryerson University, Toronto, Canada M5B 2J1
Email: bbalendr@ee.ryerson.ca

Received 19 March 2004; Revised 5 November 2004

Infrared has abundant, unregulated bandwidth enabling rapid deployment at low cost. However, safety limits on power emission levels (IEC825), large noise due to ambient lighting, and multipath dispersion remain as hurdles in diffused indoor environments. Especially, the high-frequency periodic interference produced by fluorescent lights is a major concern. Spread spectrum techniques enable low-power operation and noise rejection, at the expense of large processing gain. In this paper, we quantify the noise received and propose an adaptive FIR filter to *jointly* cancel the multipath dispersion and the fluorescent light noise in an infrared CDMA system. From analytical and simulation results, the adaptive filter significantly enhances the noise rejection capability of the CDMA system and tracks well the quasistationary indoor wireless channel. Our results show tenfold improvement in the BER for a given SNR and processing gain due to the adaptive filter. The filter also performs well in the multiuser environment.

Keywords and phrases: optical wireless, adaptive filters, equalization, noise cancellation, infrared.

1. INTRODUCTION

The history of optical wireless communications (free space optical links) predates that of fiber optics. Optical wireless communication is in use today in many applications, offering very-high-speed wireless links cost-effectively. Wireless communications based on infrared (IR) technology is one of the most growing areas in telecommunications.

IEEE has specified IR as one of the physical layer options for 802.11 [1]. IR is the least researched option in 802.11 although it has plenty of potential. IR spectrum lying in the THz range does not fall under FCC regulations and there is no electromagnetic interference (EMI) with radio systems. As a result, IR offers an unregulated huge bandwidth for high-speed wireless multimedia. Since, IR is confined within a room, the indoor IR links are secure against casual eavesdropping. This also means that the same optical wavelength can be reused in adjacent rooms without interference. Moreover, high-speed IR emitters and detectors are available nowadays at relatively low cost.

1.1. Dispersion

Indoor IR wireless systems can have diffuse or point-to-point (line-of-sight) architectures [2]. IrDA, supporting up to 16 Mb/s, is a good example for line-of-sight architecture. Even 155 Mb/s line-of-sight link is demonstrated using bootstrapped APD and holographic transmitter [3]. However, diffuse links are preferred for wireless LAN-type service because of the flexibility and robustness. With the diffuse channel, there is no need for accurate alignment between the transmitter and the receiver. The main drawback of the diffuse system is the temporal dispersion caused by reflections. In addition, the transmitted power should be much larger in a diffused system because the entire room cavity needs to be filled with IR energy [4]. However, since the square law photo detector is much larger than the IR wavelength, multipath propagation does not produce fading in an intensity-modulated direct detected (IM/DD) system; it causes only additive intersymbol interference [2].

There are several attempts made in a diffuse environment to provide high-speed access. Tang et al. investigated multibeam transmitters for angular and imaging diversity [5]; parallel transmission using multiple subcarriers similar to OFDM is investigated in [6]; the necessity of an equalizer to alleviate multipath effects above 10 Mb/s is indicated

in [7]; equalization of OOK-CDMA systems is investigated in [8]. Marsh and Kahn have shown even with equalization, the system performance severely degrades above 50 Mb/s [9].

1.2. Noise

Another major concern with in-building IR systems is the ambient light that also has significant energy in the IR band. Although out-of-band optical power can be filtered using fixed optical filters, in-band noise remains an issue. The Sun as well as fluorescent and incandescent lamps emit IR noise. Out of these, fluorescent lights with electronic ballasts are the major concern for optical wireless systems [10]. Due to the high-frequency switching of these electronic ballasts, noise spectrum extends up to 1 MHz. This poses more serious impairment and cannot be normally filtered out using electrical highpass filters [11].

Different techniques for noise cancellation have been tried: adaptive noise cancellation technique that is relatively flexible and robust is investigated in [12] and receiver design optimization is described in [13].

The SNR cannot be arbitrarily increased in this scenario by increasing the signal power. Regulatory bodies like IEC825 control the emission level of IR energy to protect human eye and skin. Detectors with large photosensitive area will collect more IR energy and increase the SNR. However, detector junction capacitance, which increases with the photosensitive area, limits the data rate in this case [14]. The SNR under different multiple access scenarios is also investigated in [15, 16].

From the foregoing, it is clear that advanced signal processing techniques are needed to provide high-speed diffuse wireless services in the IR band. The key concerns are (1) meeting the IEC825 power emission requirements, (2) overcoming the large noise power due to the ambient lighting, and (3) equalizing for the multipath dispersion in real time.

1.3. Infrared CDMA

IR-CDMA provides an attractive solution in this scenario because CDMA technique inherently enables low-power operation at an expense of reduced bit rate [17]. In [18], it has been shown that IR-CDMA using optical orthogonal codes (OOC) can operate at power levels well below ambient light power levels. However, a large bandwidth is required in these systems because of the sparse nature of length of the OOC. Marsh and Kahn [15] compared multitude of multiple access techniques and concluded that, for cells with radii below 1.5 m, only CDMA with m-sequence does not develop an irreducible BER and is therefore the only choice.

CDMA can be either on-off keyed (OOK-CDMA) or pulse-position modulated (PPM-CDMA). Matsuo et al. [19] showed that OOK-CDMA performs better than simple OOK at low transmission power assuming OOC. PPM-CDMA provides an improvement in bit rate according to Elmirghani and Cryan, compared to OOK-CDMA [20].

Some work especially targets the impairment due to electronic ballast. The authors of [10] evaluated the performance of OOK and PPM infrared links in the presence of electronic ballast interference and dispersion, and found PPM less susceptible than OOK to fluorescent lighting, particularly at high bit rates. They have shown that a first-order highpass filter is not effective in OOK systems, however, such a filter is useful in PPM systems.

O'Farrell and Kiatweerasakul have investigated the performance of an IR sequence inverse keyed (SIK) OOK-CDMA system under fluorescent light interference and line-of-sight channel [21]. They showed the fluorescent light interference is reduced by (de)spreading at the receiver. This is due to the inherent noise rejection and antijamming capabilities of CDMA. However, large processing gain is needed in order to sufficiently reject the high-power fluorescent light interference [21]. This will limit the useful bit rate. The same system under multipath dispersion and artificial light interference is investigated in [22]. Results again indicate that small power penalties incurred due to dispersion and electronic ballast interference somewhat affect the system.

From the foregoing, previous work can be categorized into three groups:

(i) inherent performance improvement due to spread spectrum techniques (either PPM or OOK),
(ii) stand-alone equalization techniques,
(iii) stand-alone noise cancellation techniques.

In this paper, we pick an IR SIK-CDMA system that already has good noise/dispersion performance, and introduce an additional adaptive filter (AF) at the receiver front end to *jointly* equalize and to denoise. The joint approach significantly improves the performance with little overhead. Analytical and simulation results show the system BER can be decreased by 10–12 times for a given chip rate and SNR with the AF. This significant increase is largely contributed to the periodic fluorescent light interference suppression by the AF. The recursive least square (RLS) AF is also able to track the quasistationary indoor channel in real time.

The outline of the paper is as follows: system, channel, and noise models as well as spectral considerations used in the study are described in Section 2. Mathematical derivations and the system analysis are described in Section 3. Simulation model, parameters, and results are described in Section 4. Section 5 concludes the paper with discussion.

2. SYSTEM, NOISE, AND CHANNEL MODELS

We consider an indoor diffuse LAN environment where multitude of portable units simultaneously and asynchronously communicate with each other using direct sequence CDMA technique. Typically the units are on table tops and radiate towards the ceiling that acts as the reflector, and receive the reflected signal. We consider OOK modulation and SIK spreading. There are multitude of fluorescent lights in this typical office room.

2.1. The indoor wireless infrared channel

Several techniques have been proposed for characterizing the indoor optical wireless channel [23]. Dependency on the

physical dimensions of a particular indoor environment prevents the generality of these models. However, Carruthers and Khan [2] showed that nondirected IM/DD channels can be characterized solely by their path loss and delay spread due to the strong correlation between multipath power requirement and delay spread for baseband modulation schemes (OOK and PPM). This gives us a uniform and reproducible method to evaluate the performance. These general models have been used by many authors afterwards [19]. These are

(1) exponentially decaying channel model that represents most line-of-sight links,
(2) ceiling bounce channel model that is suitable for diffuse systems.

The ceiling bounce diffuse channel model is adopted in this research work. The impulse response $h(t,a)$ of the ceiling bounce channel as given in [2] is

$$h(t,a) = G_0 \cdot \frac{6a^6}{(t+a)^7} \cdot u(t), \tag{1}$$

where

$$a = \frac{2H}{c}, \qquad G_0 = \frac{\rho \cdot A_r}{3\pi \cdot H^2}. \tag{2}$$

Here, $u(t)$ is the unit step function, H is the height of the ceiling above the transmitter and receiver, ρ is the reflectivity of the reflecting surface, A_r is the receiver photo diode area, and c is speed of light.

2.2. Fluorescent light periodic interference

Interference from fluorescent lights has been identified as the biggest concern for indoor IR systems [24]. There are two types of ballasts used in fluorescent lights. The conventional ballasts switch at power line frequency (60 Hz), therefore, together with their harmonics, they interfere with the IR systems at 60 Hz. This low-frequency interference can be removed by electrical highpass filters after the photo detector. However, electronic ballasts are mostly used in fluorescent lights nowadays. These electronic ballasts switch at high frequencies (typically at 37.5 kHz), and the harmonics extend up to MHz range. This will spectrally overlap with our frequency of interest and electrical highpass filtering is not much useful.

Recently, several researchers looked at the situation. Moreira et al. in [11] did extensive measurements and proposed a mathematical model for the periodic nature of the interference from the electronic ballast fluorescent light. We use this model to synthesize the fluorescent light interference in this paper. This model is

$$\begin{aligned} m(t) = RP_m + \frac{RP_m}{K_1} \sum_{i=1}^{20} \left[b_i \cos\left(2\pi(100i-20)t + \xi_i\right) \right. \\ \left. + c_i \cos\left(2\pi 100 i + \varphi_i\right) \right] \\ + \frac{RP_m}{K_2} \left[d_0 \cos\left(2\pi f_h t + \theta_0\right) + \sum_{j=1}^{11} \cos\left(2\pi 2j f_h t + \theta_j\right) \right], \end{aligned} \tag{3}$$

where $K_1 = 5.9$ and $K_2 = 2.1$, R is the responsivity of the photodiode, and P_m is the average optical power of the interfering signal. $f_h = 37.5$ kHz is the fundamental frequency of the electronic ballast. The first, second, and third terms of (3) represent the photo currents due to the mean fluorescent power, the low-frequency, and high-frequency components, respectively. The parameters b_i and c_i are estimated and given in [11].

2.3. Other noise processes

Other than the periodic interference described above, the shot noise due to ambient light is the predominant noise in an IR wireless receiver. This relatively static noise power can be written as

$$P_{\text{AWGN}} = 2qRP_mB, \tag{4}$$

where q is the charge of an electron, B is the bandwidth of interest, P_m is the mean received optical power, and R is the responsivity of the detector.

2.4. Spectral consideration

Typically indoor lights emit much higher optical power compared to IR transmitters. This nature has the potential to affect the system performance severely. Fortunately however, not all the optical power emitted by these lights is received by the photo detector. Only a fraction of the power is actually received. This happens due to both spectral and spatial mismatch. The spectral issue is discussed in this section and the actual power received is estimated. The spatial issue is discussed in the next section.

Figure 1 shows the spectrum of light emitted from fluorescent lights. This graph is created by using the measurements in [25]. Figure 1 shows that the major portion of the fluorescent light output power is visible light (between 400–700 nm). However, there is some IR energy that concerns us. If we assume a silicon photodiode, it has peak responsivity at 900 nm [26] and is not very sensitive in the visible band. We superimposed the responsivity curve of a typical Si photodiode to show the overlapping area in Figure 1. From the graph it can be seen that most of the emitted power falls out of the operating wavelength of the photo detector.

The responsivity of a Si photodiode [26] is quantitatively shown by

$$\Re = \frac{\eta q \lambda}{hc}, \tag{5}$$

where η is the quantum efficiency, λ is the wavelength, h is Planck's constant, and c is the speed of light. From (5), the responsivity of a given photodiode increases with the wavelength until the upper cutoff wavelength λ_c. The upper cutoff wavelength λ_c depends on the band gap energy of the semiconductor material, $\lambda_c = 1100$ nm for Si. At very low wavelengths, the recombination time of the electron-hole pairs is too short to generate photo current and the responsivity will be too low.

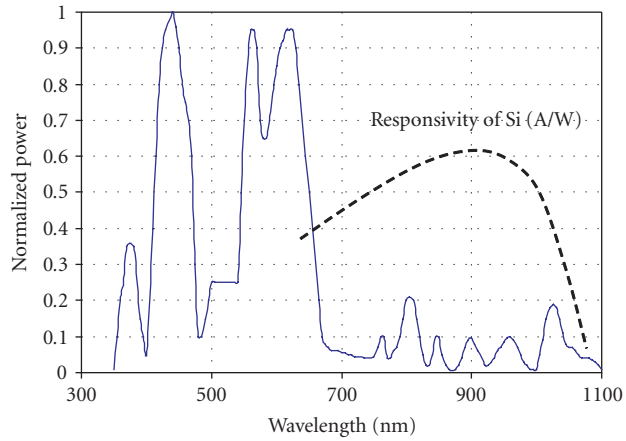

Figure 1: Spectral distribution of the fluorescent light output noise power; superimposed is the responsivity of Si.

We estimated the fraction of the optical power that will actually be received by integrating the overlapping area.[1] From this, around 12 % of the fluorescent power is actually received by a Si photodiode[2] due to spectral mismatch.

2.5. Field of view consideration

Only a portion of the power from the fluorescent light will be received by the photodiode depending on the receiver area A_r and receiver field of view (FOV) as well.

To estimate this, we assume that the room cavity is uniformly illuminated using evenly spaced multitude of fluorescent light. This is typical in modern offices. In this scenario, all the walls and ceiling would be reflecting the light and acting as Lambertian surfaces. If the power emitted per surface area of the room (radiant emittance) is ω, then the received power is given as (6). The proof is given in [4].

$$P_m = \omega A_r \sin^2(\text{FOV}). \tag{6}$$

3. SIGNAL-TO-NOISE-AND-INTERFERENCE RATIO

In this section, we derive a mathematical expression for the signal-to-noise-and-interference ratio (SINR). This is done considering the standard spread spectrum system without the AF first, and then the same system with the AF (Figure 3). These two derivations enable comparative evaluation.

3.1. Standard CDMA system with fluorescent light interference

Figure 2 shows the multiuser CDMA environment, where $g_k(t)$ is the signature waveform of the kth user with chip period T_c, I_k is wide sense stationary process with mean μ, $h(t)$

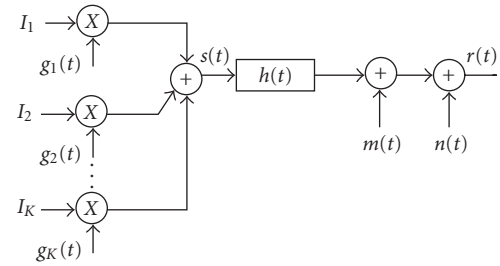

Figure 2: Multiuser optical wireless CDMA system.

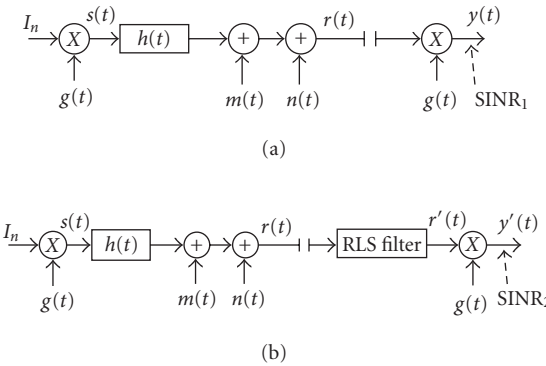

Figure 3: Simplified block diagram of the optical wireless CDMA systems (a) without the adaptive filter and (b) with the adaptive filter.

is impulse response of the channel, $m(t)$ is the periodic interference of the electronic ballast fluorescent lights, and $n(t)$ is the additive Gaussian noise.

Figure 3a shows the simplified block diagram of the standard IR-CDMA link per one user. I_n is the baseband digital data emerging from the user. The spreading sequence $g(t)$ is given by

$$g(t) = \sum_{i=0}^{N-1} a(i)p(t - iT_c), \quad a(i) \in (1, 0), \tag{7}$$

where $a(i)$ is the unipolar PN sequence, $p(t)$ is the pulse shape, and T_c is the chip period. N is the code length, so that each bit has N chips ($NT_c = T$). The information sequence I_n is combined with the signature waveforms $g(t)$ to spread the transmitted signal. Assuming the system has K users, the kth-user signal is $s_k(t)$ and the total received signals $s(t)$ are

$$s(t) = \sum_{k=1}^{K} s_k(t) = \sum_{k=1}^{K} \sum_{j=-\infty}^{\infty} \sqrt{\varepsilon_k} \cdot I_k \circ g(t - jT). \tag{8}$$

Here, ε_k is the energy of the kth pulse and $\circ$ is the SIK operator. According to SIK, the PN sequence is transmitted for data "1" and the inverse of the PN sequence is transmitted for data "0."

We use the frequency domain approach for compact derivation. Hence, the power spectral density (PSD) $\phi_{ss}(f)$

[1] The estimation is done without assuming any optical bandpass filters. Optical filters would further reduce the power received.

[2] Si photodiode gives a worst-case estimate because its responsivity range is 450 nm–1100 nm. Ge or InGaAs detectors will receive even less fluorescent light noise, but they are more susceptible to incandescent light noise.

of the signal $s(t)$ is [27]

$$\phi_{ss}(f) = \sum_{k=1}^{K} \frac{1}{T} |G(f)|^2 \cdot \phi_{ii}(f), \tag{9}$$

where $G(f)$ is the Fourier transform of $g(t)$ and $\phi_{ii}(f)$ is the PSD of the information sequence I_n. From Figure 3, the signal received at the receiver before despreading is

$$r(t) = s(t) * h(t) + n(t) + m(t), \tag{10}$$

where the notation asterisk denotes the convolution operation. The PSD of the output signal $r(t)$ is

$$\phi_{rr}(f) = \phi_{ss}(f)|H(f)|^2 + \phi_{nn}(f) + \phi_{mm}(f), \tag{11}$$

where $H(f)$ is the Fourier transform of the channel impulse response $h(t)$, $\phi_{nn}(f)$ is the PSD of the Gaussian noise, and $\phi_{mm}(f)$ is the PSD of the fluorescent interference. Note that the multipath dispersion affect is included in (11) because it is embedded in $H(f)$. Therefore, the PSD of the output signal $y(t)$ after despreading is given as

$$\phi_{yy}(f) = \frac{1}{T}|G(f)|^2 \left\{\phi_{ss}(f)|H(f)|^2 + \phi_{nn}(f) + \phi_{mm}(f)\right\}. \tag{12}$$

We assume kth user is our required user, therefore in a multiuser environment, the PSD $\phi_{ss}(f)$ in (9) can be rearranged as the desired user signal and the interference signals, respectively, as

$$\begin{aligned}\phi_{ss}(f) &= \frac{1}{T}|G_k(f)|^2 \phi_{i_k i_k}(f) \\ &\quad + \frac{1}{T}\sum_{\substack{n=1 \\ n\neq k}}^{K} |G_n(f)|^2 \phi_{i_n i_n}(f), \quad n,k \in (1,K),\end{aligned} \tag{13}$$

where $\phi_{i_k i_k}(f)$ is the PSD of the kth-user information sequence and $\phi_{i_n i_n}(f)$ is the PSD of other users' information sequence. $G_k(f)$ and $G_n(f)$ are the Fourier transforms of the signature waveforms of the kth and nth users, respectively. Then, substituting (13) into (12) the PSD of the interference signal can be written as

$$\begin{aligned}&\phi_{\text{interference}}(f) \\ &\quad = \sum_{\substack{n=1 \\ n\neq k}}^{K} \frac{1}{T^2}|G_k(f)|^2 |G_n(f)|^2 \phi_{i_n i_n}(f)|H(f)|^2.\end{aligned} \tag{14}$$

Therefore, the multiuser interference power is given by integrating the PSD over the entire spectrum [27]. This is given in (15), where R is the responsivity of the photodiode:

$$\begin{aligned}&P_{\text{interference}} \\ &\quad = \frac{R^2}{T^2}\int_{-\infty}^{\infty} \sum_{\substack{n=1 \\ n\neq k}}^{K} |G_k(f)|^2 |G_n(f)|^2 \phi_{i_n i_n}(f)|H(f)|^2 df.\end{aligned} \tag{15}$$

Similarly from (12) and (13), the desired (kth) user power is

$$P_{\text{required}} = \frac{R^2}{T^2}\int_{-\infty}^{\infty} |G_k(f)|^4 \cdot |H(f)|^2 \cdot \phi_{i_k i_k}(f) df. \tag{16}$$

The Gaussian distributed noise power is

$$P_{\text{AWGN}} = R^2 \int_{-\infty}^{\infty} \frac{1}{T}|G(f)|^2 \phi_{nn}(f) df, \tag{17}$$

where $\int_{-\infty}^{\infty} \phi_{nn}(f) df = 2qRP_mB$.

The periodic fluorescent light interference power is

$$P_{\text{fluorescent}} = R^2 \int_{-\infty}^{\infty} \frac{1}{T}|G(f)|^2 \phi_{mm}(f) df. \tag{18}$$

However, we can find the fluorescent interference power using Moreira's model given in (3). This is given as follows:

$$\begin{aligned}&\int_{-\infty}^{\infty} \phi_{mm}(f) df \\ &\quad = \frac{R^2 P_m^2}{N^2}\left\{\frac{1}{2K_1^2}\sum_{i=1}^{20}(a_i^2 + b_i^2) + \frac{1}{2K_2^2}\sum_{j=1}^{11}(d_j^2 + d_0^2)\right\}.\end{aligned} \tag{19}$$

Furthermore, the numerical values of the parameters a_i, b_i, and d_j are estimated in [11]. These values can be used to further simplify (19) as

$$\int_{-\infty}^{\infty} \phi_{mm}(f) df = \frac{R^2 P_m^2}{N^2} \cdot (0.3593)^2, \tag{20}$$

where P_m is the average optical power of the interference signal (that is derived in (6) in Section 2.5), and N is the CDMA spreading gain.

Finally the system SINR is

$$\text{SINR}_1 = \frac{P_{\text{required}}}{P_{\text{interference}} + P_{\text{fluorescent}} + P_{\text{AWGN}}}. \tag{21}$$

When there is no multiuser interference, this reduces to

$$\text{SNR}_1 = \frac{P_{\text{required}}}{P_{\text{fluorescent}} + P_{\text{AWGN}}}. \tag{22}$$

3.2. Improved SINR with the adaptive filter

In this section, the system performance with the AF is analyzed. For this, we include a discrete time AF just before despreading as shown in Figure 3b. The RLS adaptive algorithm is considered in this analysis. The RLS algorithm keeps the training sequence short and is preferred with nonstationary and non white inputs.

The AF is trained with a training sequence first. During training, input to the AF $r(n)$ is the training sequence corrupted with noise ($r(n) = s(n) * h(n) + m(n) + n(n)$) and the desired response $d(n)$ is the training sequence ($d(n) = s(n)$). The objective of the AF is to update the tap coefficients $w(n)$ on a sample-by-sample basis so that the estimation error between desired output and estimated output is minimized in

a mean square sense. The step-by-step RLS algorithm is described in [28] and not repeated here. The optimum value of the tap weight w_{op} for the RLS filter can be determined using Wiener-Hopf normal equation that is given as

$$w_{\text{op}}(n) = \phi^{-1}(n)\theta(n), \tag{23}$$

where $\phi(n)$ is the $m \times m$ time-averaged correlation matrix of the input to the AF, and $\theta(n)$ is the $m \times 1$ time-averaged cross correlation vector between the desired response and the input:

$$\phi(n) = \sum_{i=1}^{m} r(i)r(i)^T,$$
$$\theta(n) = \sum_{i=1}^{m} r(i)d(i) = \sum_{i=1}^{m} \{s(i) * h(i) + m(i) + n(i)\}s(i). \tag{24}$$

Therefore, the optimal filter weight depends on three things: (1) the channel matrix, (2) correlation between the periodic interference $m(i)$ and the signal $s(i)$, and (3) correlation between the Gaussian noise $n(i)$ and $s(i)$.

We assume that the Fourier transform of AF coefficients is $W(f)$. Then the PSD of the output of the AF $r'(t)$ in Figure 3 is given as

$$\phi'_{rr}(f) = \phi_{rr}(f)\,|W(f)|^2. \tag{25}$$

Let the received signal after despreading be $y'(t)$. The power spectral density of the $y'(t)$ is

$$\begin{aligned}\phi'_{yy}(f) = {} & \frac{1}{T}\phi_{ss}(f) \cdot |G(f)|^2 \cdot |W(f)|^2 |H(f)|^2 \\ & + \frac{1}{T}|W(f)|^2 \cdot |G(f)|^2 \phi_{nn}(f) \\ & + \frac{1}{T} \cdot |W(f)|^2 \cdot |G(f)|^2 \cdot \phi_{mm}(f).\end{aligned} \tag{26}$$

Therefore, with the AF, the desired user's received power, multiuser interference power, AWGN noise power, and the fluorescent noise powers can be given as follows, respectively:

$$P_{\text{required}} = \frac{R^2}{T^2}\int_{-\infty}^{\infty} |G_k(f)|^4 \cdot \phi_{i_k i_k}(f) \cdot |W(f)|^2 \cdot |H(f)|^2 df, \tag{27}$$

$$P_{\text{interference}} = \frac{R^2}{T^2}\int_{-\infty}^{\infty} \sum_{n \neq k} \cdot |G_k(f)|^2 \cdot |G_n(f)|^2 \cdot \phi_{i_n i_n}(f) \cdot |W(f)|^2 \cdot |H(f)|^2 df, \tag{28}$$

$$P_{\text{AWGN}} = \frac{R^2}{T}\int_{-\infty}^{\infty} |G_k(f)|^2 \cdot |W(f)|^2 \cdot \phi_{nn}(f) df, \tag{29}$$

$$P_{\text{fluorescent}} = \frac{R^2}{T}\int_{-\infty}^{\infty} |G_k(f)|^2 \cdot |W(f)|^2 \cdot \phi_{mm}(f) df. \tag{30}$$

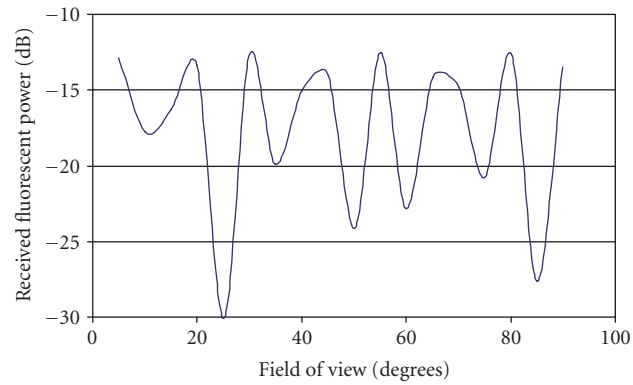

Figure 4: Received power from the ambient light as a function of the receiver's field of view.

Therefore, the improved SINR with the adaptive filter SINR_2 is

$$\text{SINR}_2 = \frac{P_{\text{required}}}{P_{\text{interference}} + P_{\text{fluorescent}} + P_{\text{AWGN}}}. \tag{31}$$

When there is no multiuser interference, this reduces to

$$\text{SNR}_2 = \frac{P_{\text{required}}}{P_{\text{fluorescent}} + P_{\text{AWGN}}}. \tag{32}$$

4. SIMULATION AND RESULTS

First, we obtained the relationship between the received fluorescent light power and the FOV using the expression in (6) and spectral considerations. This relationship is shown in Figure 4. The receiver has an area $A_r = 1\,\text{cm}^2$, responsivity of 0.62 A/W, and radiant emittance ω is 6.8×10^{-3}. The figure shows that the received light power significantly varies with the FOV. FOV = 22.5° seems to be unique angle at which the received power is minimum. This phenomenon is observed by some other researchers as well [13]. We used FOV = 22.5° in subsequent stages.

In our simulation model, the IR-CDMA system is trained using least mean square (LMS) and RLS algorithm. The Simulink running on Matlab is used to run the simulations to get the BER curves. The simulation is done by implementing Figure 3 at discrete time instances of T_c. Uncorrelated user information sequence (I_n) is generated using binary random integer generator. This data is spread using SIK technique using the built-in PN sequence generator of the Simulink.

This spread chip sequence is passed through the multipath channel next. The multipath channel is implemented by having discrete paths with delay T_c. In order to get the gains of each path, the ceiling bounce channel model of [29] is sampled at discrete time intervals T_c as follows:

$$h(nT_c) = G_0 \cdot \frac{6a^6}{(nT_c + a)^7} \times \left(1 + \frac{G_{\text{rand}}(nT_c)}{4}\right), \quad n = 1, 2, 3, \ldots. \tag{33}$$

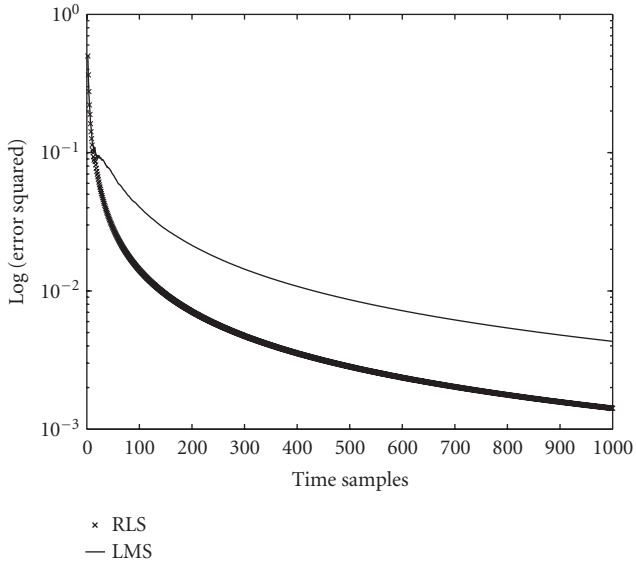

Figure 5: Learning curves with LMS and RLS adaptive algorithms at equalizer configuration.

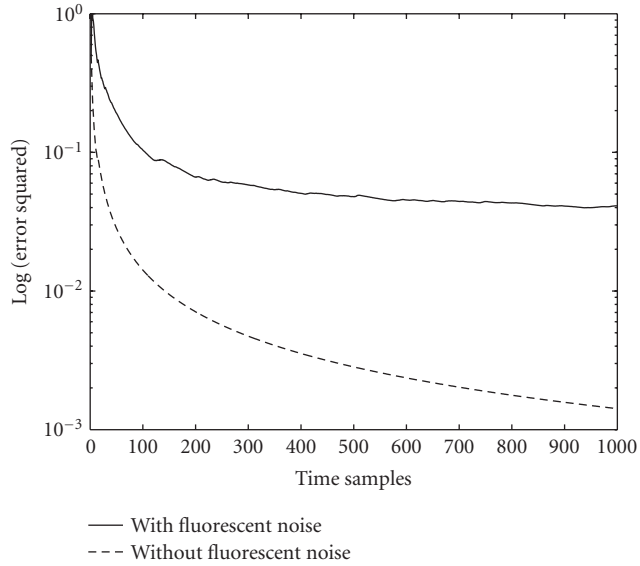

Figure 6: Learning curve of the RLS adaptive filter in the (1) equalizer configuration (dashed) and (2) equalizer and denoiser configurations (solid).

$G_{\text{rand}}(nT_c)$ is added to include the channel variations due to shadowing on top of the fixed ceiling bounce model. This gives maximum 25% variation. $a = 2H/c$, H is taken as 3.5 m, and ρ is 0.9. The number of significant paths depends on the sampling rate because the channel memory is fixed by the ceiling bounce model. We considered 3 Mb/s and $N = 15$. This gives 45 Mc/s chip rate and 22.22 nanoseconds sampling time. Hence the number of significant paths is 7.

After transmission through the multipath channel, the noise was added to the received signal. The fluorescent light noise $m(t)$ is generated in discrete time intervals T_c by sampling the noise power expression (3) in a similar manner. A Gaussian white noise $n(t)$ is also added to represent other noise processes in the system. We assumed the received power P_{required} is 1 mW per user. The noise power is adjusted accordingly to get the desired SNR.

The noisy, dispersed signal is then input to the adaptive filter. AF output and the desired sequence $d(n)$ are compared to generate the error which is fed back to the AF. The tap spacing of the AF is T_c. After the AF, the signal was despread, transmitted bit was estimated and the BER was computed.

The AF is trained until the mean squared error (MSE) reaches a reasonable minimum. In this work, learning curves are obtained with both LMS and RLS algorithms. From Figure 5 the RLS algorithm achieves smaller MSE quickly compared to the LMS algorithm. The RLS algorithm is selected due to this fast convergence.

The system is first analyzed only with multipath effect and then only with noise. Then it is tested with both the multipath dispersion and noise. The learning curves of the RLS algorithm in both cases are shown in Figure 6.

When the RLS filter is configured to equalize for the multipath dispersion only, it was found that 5 tap weights are sufficient for this purpose. The Fourier transform of these tap weights resembled that of a highpass filter, probably because the time dispersive channel resembles a lowpass filter. When the fluorescent interference is introduced to the system, the filter order is required to be high to mitigate this interference. The tap weights are significant up to filter order 15 for adequate noise suppression and equalization. Therefore, we fixed the filter order at 15.

It is seen that the minimum mean square error (MMSE) is close to 10^{-3} for only equalization. When the fluorescent noise is included, the MMSE is about 0.1. This shows that the filter struggles to cancel both the noise and the dispersion even with 15 taps (however, the BER performance still significantly improves as we see below). Nevertheless the filter converges fast; the learning curves in Figure 6 show that the AF converges well within 250 iterations as an equalizer. It converges reasonably within 200 iterations for both multipath and fluorescent noise interferences.

Frequency response of the AF under equalization and noise cancellation configuration is shown in Figure 7. The response looks like a combination of highpass and comb filters. It also cancels 75 kHz and its harmonics and has a sharp notch especially at 300 kHz.

The optimum AF weights are obtained by running the Simulink model. Then using these filter weights and equations from (27) to (30) the SNR as defined in (32) and (22) is calculated. Here, P_{required} is 1 mW. $P_{\text{fluorescent}}$ is obtained from (18) and P_{AWGN} is obtained from (17). The SNR is changed by changing the received ambient light power P_m. The pulse $g(t)$ has sinc spectrum, ϕ_{i_k,i_k} is white (pure random data), $H(f)$ is Fourier transform of $h(t)$ in (1), hence the multipath dispersion is accounted for, $\phi_{nn}(f)$ is white, and $\phi_{mm}(f)$ is the PSD of $m(t)$. Gaussian assumption (BER =

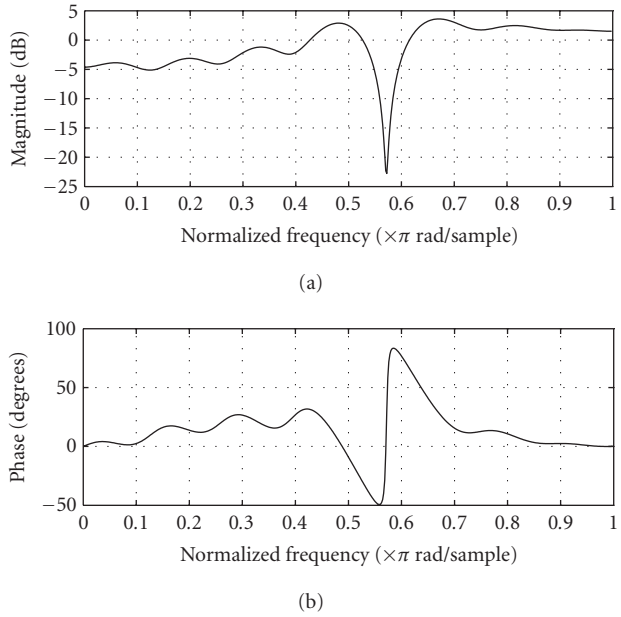

Figure 7: Frequency response of the RLS adaptive filter that compensates both multipath and fluorescent noise interference.

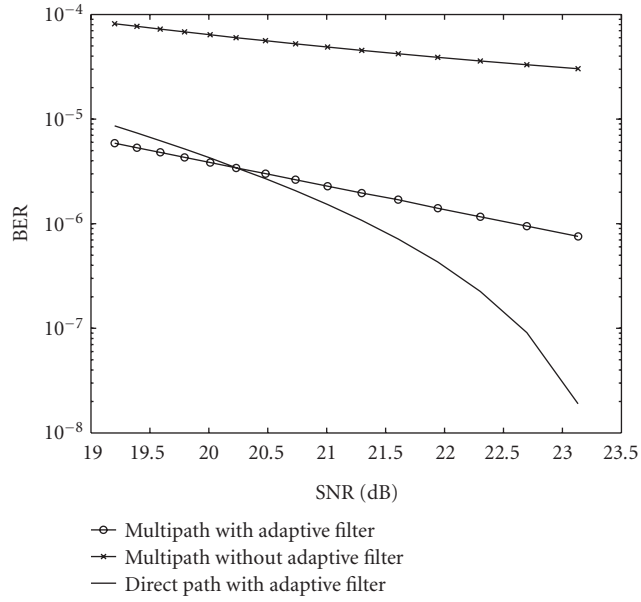

Figure 8: Estimated BER curves of the IR-CDMA system showing the improvement due to the adaptive filter ($N = 7$).

$(1/2)\text{erfc}\{\sqrt{\text{SNR}/2}\}$) is used to get Figure 8 that shows the estimated BER curves of the IR-CDMA system. Although the Gaussian assumption is not accurate when the number of fluorescent lights are small, this figure gives a ballpark estimate.

Figure 8 shows that the AF significantly improves the BER of the IR-CDMA system, even with multipath dispersion. In the direct path case, the BER really goes down when SNR $\geq$ 21 dB. This is because, in this case, the AF has to train itself for noise cancellation only. With multiple paths, even if the SNR is high, dispersion limits the performance. Gaussian assumption is used for the noise statistics to estimate the BER curves in this figure. This assumption is discussed in Section 5.

Figure 9 shows the simulated BER curves for a single user. The filter weights were obtained by transmitting a known training sequence first. Then the filter weights were frozen, and unknown data is transmitted to compute the BER. In real systems this training sequence needs to be periodically transmitted. Similar to the calculated results, simulation results also show that the AF improves the BER by about ten times under noise and multipath interference. However, the direct path and multipath curves are closer for some reason.

Figure 10 shows the simulated BER curves with one and two users. Processing gain $N = 15$, AF with 15 taps is used. Multipath gains are obtained from (33). Equal power of 1 mW is received from both users. The users use the delayed versions of the maximal length sequence of length 15. The figure clearly shows that the AF is improving the performance with both one and two users. Single-user performance without the AF is worse than two users with AF.

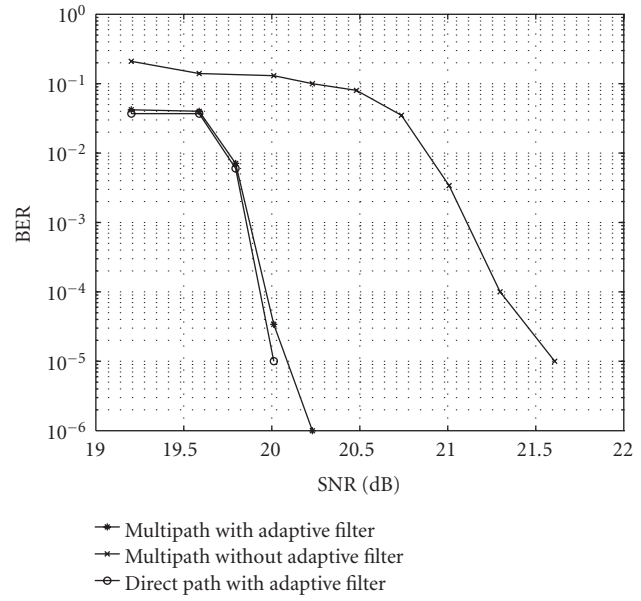

Figure 9: Simulated BER curves of the IR-CDMA system showing the improvement due to the adaptive filter ($N = 7$).

Finally, Figure 11 shows how the adaptive filter is able to track channel variations. Initially, when the shadowing factor is zero the filter converges in about 120 samples, then as the factor jumps to -1, it still reasonably converges in about 100 samples, when the channel takes a large jump from -1 to $+1$ (worst case change), it takes little longer for the initial convergence; still it reaches MSE $\approx 10^{-1}$ within 100 samples. At a chip rate of 45 Mc/s, this corresponds to 2.22 microseconds. This time favorably compares with the coherent time of an indoor wireless channel.

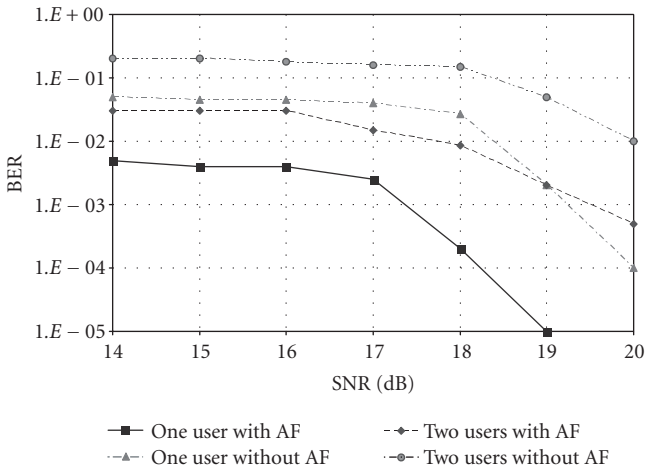

Figure 10: Simulated BER curves of the IR-CDMA system with adaptive filter under multiuser conditions ($N = 15$).

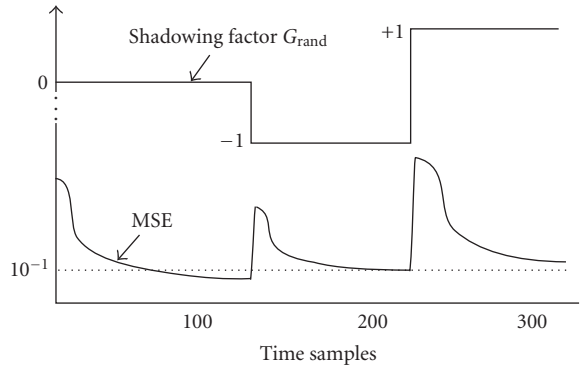

Figure 11: Tracking pattern of the adaptive filter with the channel change.

5. CONCLUSION AND DISCUSSION

In this paper, we present the performance improvement due to the deployment of an AF in diffuse indoor wireless CDMA system. The analysis is done mathematically and subsequently the technique is tested in a simulation model. Both the analytical and simulation results agree and show that the AF improves the BER of the IR-CDMA system by tenfold. In the direct path condition, the improvement is even better. The given improvement is obtained with the AF running at the chip rate. Higher sampling rates and fractional delay filters will further improve the performance.

Adaptive digital noise cancellation techniques are seldom used in wireless communication systems, because of the low level of noise and slow convergence of adaptive algorithms. Nevertheless, indoor IR environment provides a unique challenge because of the large ambient noise; this could make the SNR even negative sometimes. The proposed adaptive denoising technique is useful in this scenario.

The indoor wireless systems are quasistationary systems in general. Furthermore, because of the short distance and fixed locations of the noise sources the optical wireless channel seems to vary very slowly. The RLS algorithm seems to converge well within the coherent time of the channel (Figure 11). This makes our solution practical. However, the training sequence that needs to be periodically transmitted will moderately decrease the channel capacity because of the additional overhead.

The frequency spectrum of the AF gives an insight. The filter trains itself resembling a comb filter and cancels out the frequencies of 37.5 kHz and its harmonics. However, it has strong notch at 300 kHz in which the phase also reverses. We believe the reason for this has more to do with how the fast Fourier transform (FFT) algorithm works in Matlab software and limited number of AF taps. This notch decreases in magnitude when number of filter taps are large.

Gaussian assumption used to obtain Figure 8 is not quite accurate. However, no major conclusion is drawn from this figure. Major results obtained in the paper (Figures 9, 10, and 11) are based on simulation that also agree with Figure 8. Getting exact statistics in the presence of Poisson distributed quantum noise, periodic interference with multitude of frequencies, and nonstationary ambient noise would be too involved and we doubt it would serve much to the overall purpose of the paper.

In future work, we can consider a single filter which can do despreading, equalization, and noise cancellation jointly. This will further reduce the complexity of the receiver.

REFERENCES

[1] R. T. Valadas, A. R. Tavares, A. M. de Oliveira Duarte, A. C. Moreira, and C. T. Lomba, "The infrared physical layer of the IEEE 802.11 standard for wireless local area networks," *IEEE Communications Magazine*, vol. 36, no. 12, pp. 107–112, 1998.

[2] J. B. Carruthers and J. M. Kahn, "Modeling of nondirected wireless infrared channels," *IEEE Transactions on Communications*, vol. 45, no. 10, pp. 1260–1268, 1997.

[3] M. J. McCullagh and D. R. Wisely, "155 Mbit/s optical wireless link using a bootstrapped silicon APD receiver," *Electronics Letters*, vol. 30, no. 5, pp. 430–432, 1994.

[4] F. R. Gfeller and U. H. Bapst, "Wireless in-house data communication via diffuse infrared radiation," *Proceedings of the IEEE*, vol. 67, no. 11, pp. 1474–1486, 1979.

[5] A. P. Tang, J. M. Kahn, and K. P. Ho, "Wireless infrared communication links using multi-beam transmitters and imaging receivers," in *Proc. IEEE International Conference on Communications*, vol. 14, pp. 180–186, Dallas, Tex, USA, June 1996.

[6] J. B. Carruthers and J. M. Kahn, "Multiple-subcarrier modulation for nondirected wireless infrared communication," *IEEE Journal on Selected Areas in Communications*, vol. 14, no. 3, pp. 538–546, 1996.

[7] K.-C. Chen, "Indoor high speed wireless networks via optical transmission," Tech. Rep., IBM Thomas J. Watson Research Center, Yorktown, Va, USA, 1994.

[8] T. Ohtsuki, H. Yamaguchi, R. Matsuo, and I. Sasase, "Equalization for infrared wireless systems using OOK-CDMA," *IEICE Transactions on Communications*, vol. E85-B, no. 10, pp. 2292–2299, 2002.

[9] G. W. Marsh and J. M. Kahn, "Performance evaluation of experimental 50-Mb/s diffuse infrared wireless link using on-off keying with decision-feedback equalization," *IEEE Transactions on Communications*, vol. 44, no. 11, pp. 1496–1504, 1996.

[10] R. Narasimhan, M. D. Audeh, and J. M. Kahn, "Effect of electronic-ballast fluorescent lighting on wireless infrared links," in *Proc. IEEE International Conference on Converging Technologies for Tomorrow's Applications (ICC '96)*, vol. 2, pp. 1213–1219, Dallas, Tex, USA, June 1996.

[11] A. J. C. Moreira, R. T. Valadas, and A. M. de Oliveira Duarte, "Optical interference produced by artificial light," *Wireless Networks*, vol. 3, no. 2, pp. 131–140, 1997.

[12] X. N. Fernando, S. Krishnan, H. Sun, and K.-M. Kamyar, "Adaptive denoising at infrared wireless receivers," in *Proc. 17th Annual AeroSense Symposium of the Infrared Technology and Applications XXIX*, B. F. Andresen and G. F. Fulop, Eds., vol. 5074 of *Proceedings of the SPIE*, pp. 199–207, Bellingham, Wash, USA, September 2003.

[13] A. J. C. Moreira, R. T. Valadas, and A. M. de Oliveira Duarte, "Reducing the effects of artificial light interference in wireless infrared transmission systems," in *IEE Colloquium on Optical Free Space Communication Links*, vol. 1, pp. 501–510, London, UK, February 1996.

[14] J. M. Senior, *Optical Fiber Communications: Principles and Practice*, Prentice-Hall, Upper Saddle River, NJ, USA, 2nd edition, 1992.

[15] G. W. Marsh and J. M. Kahn, "Channel reuse strategies for indoor infrared wireless communications," *IEEE Transactions on Communications*, vol. 45, no. 10, pp. 1280–1290, 1997.

[16] G. W. Marsh, *High-speed wireless infrared communication links*, Ph.D. thesis, University of California, Berkeley, Calif, USA, December 1995.

[17] X. N. Fernando, "Performance of an infrared wireless CDMA system," in *Proc. 17th Annual AeroSense Symposium of the Digital Wireless Communications Conference V*, vol. 5100 of *Proceedings of the SPIE*, pp. 204–214, Orlando, Fla, USA, April 2003.

[18] S. Zahedi, J. A. Salehi, and M. Nasiri-Kenari, "A photon counting approach to the performance analysis of indoors wireless infrared CDMA networks," in *Proc. IEEE 11th International Symposium on Personal, Indoor and Mobile Radio Communications (PIMRC '00)*, pp. 928–932, London, UK, September 2000.

[19] R. Matsuo, M. Matsuo, T. Ohtsuki, T. Udagawa, and I. Sasase, "Performance analysis of indoor infrared wireless systems using OOK CDMA on diffuse channels," in *Proc. IEEE Pacific Rim Conference on Communications, Computers and Signal Processing*, vol. 1, pp. 30–33, Victoria, BC, Canada, August 1999.

[20] J. M. H. Elmirghani and R. A. Cryan, "Indoor infrared wireless networks utilising PPM CDMA," in *Proc. IEEE International Conference on Communications Singapore (ICCS '94)*, pp. 334–337, Singapore, 1994.

[21] T. O'Farrell and M. Kiatweerasakul, "Performance of a spread spectrum infrared transmission system under ambient light interference," in *Proc. IEEE 9th International Symposium on Personal, Indoor and Mobile Communications*, vol. 2, pp. 703–707, Boston, Mass, USA, September 1998.

[22] K. K. Wong, T. O'Farrell, and M. Kiatweerasakul, "Infrared wireless communication using spread spectrum techniques," *IEE Proceedings Optoelectronics*, vol. 147, no. 4, pp. 308–314, 2000.

[23] J. R. Barry, J. M. Kahn, W. J. Krause, E. A. Lee, and D. G. Messerschmitt, "Simulation of multipath impulse response for indoor wireless optical channels," *IEEE Journal on Selected Areas in Communications*, vol. 11, no. 3, pp. 367–379, 1993.

[24] A. J. C. Moreira, R. T. Valadas, and A. M. de Oliveira Duarte, "Characterisation and modeling of artificial light interference in optical wireless communication systems," in *Proc. IEEE Personal, Indoor and Mobile Radio Communications (PIMRC '95)*, vol. 1, pp. 326–331, Toronto, Canada, September 1995.

[25] J. R. Barry, *Wireless Infrared Communication*, Kluwer Academic Publishers, Boston, Mass, USA, 1st edition, 1994.

[26] G. Keiser, *Optical Fiber Communications*, McGraw-Hill Higher Education, New York, NY, USA, 3rd edition, 2000.

[27] J. G. Proakis, *Digital Communications*, McGraw-Hill, New York, NY, USA, 3rd edition, 1995.

[28] S. Haykin, *Adaptive Filter Theory*, Prentice-Hall, Upper Saddle River, NJ, USA, 2002.

[29] J. M. Kahn, J. R. Barry, M. D. Audeh, J.B. Carruthers, W. J. Krause, and G. W. Marsh, "Non-directed infrared links for high-capacity wireless LANs," *IEEE Personal Communications*, vol. 1, no. 2, pp. 12–25, 1994.

Xavier N. Fernando obtained his B.Eng. (first-class honors) degree from Peradeniya University, Sri Lanka, where he was the first out of 250 students. He got a Master's degree from the Asian Institute of Technology, Bangkok, and a Ph.D. degree from the University of Calgary, Canada, in affiliation with TRLabs. He worked for AT&T for three years as an R&D Engineer. Currently he is an Assistant Professor at Ryerson University, Toronto, Canada. Dr. Fernando has one US patent and about 30 peer-reviewed publications in journals and conference proceedings. His research focuses on signal processing for cost-effective broadband multimedia delivery via optical wireless networks. Dr. Fernando's work won the Best Research Paper Award in the Canadian Conference of Electrical and Computer Engineering for year 2001. His student projects won both the first and second prizes at Opto Canada—the SPIE regional conference in Ottawa in 2002. He is a Senior Member of IEEE, a Member of SPIE, a Vice Chair of the IEEE Communications Society Toronto Chapter, and a licensed Professional Engineer in Ontario, Canada. He has many research grants including grants from the Canadian Foundation of Innovations (CFI), Ontario Innovations Trust (OIT), and the Natural Sciences and Engineering Research Council (NSERC) of Canada.

Balakanthan Balendran obtained his Bachelor's degree in electrical and electronic engineering in Sri Lanka in 1995. He then worked as a Telecommunication Engineer in Sri Lanka for 5 years and as a Customer Service Engineer for 2 years at NCR Canada, Toronto. He obtained his Master's degree at Ryerson University, Toronto, Canada, in 2004. The thesis topic was "Adaptive signal processing for infrared wireless CDMA systems." His research area is optical communications. He received Ryerson's Graduate Scholarship in electrical and computer engineering for 2003/2004. Currently he is working as an Assistant General Manager for the Telecommunication Engineering Division of Sierra Construction Ltd., Sri Lanka.